The Astrophysical Journal, 842:111 (11pp), 2017 June 20 https://doi.org/10.3847/1538-4357/aa6f61

Implications of the Low Binary Black Hole Aligned Spins Observed by LIGO

Kenta Hotokezaka[1,2] and Tsvi Piran[2]
[1] Center for Computational Astrophysics, Flatiron Institute, 162 5th Avenue, New York, NY 10010, USA
[2] Racah Institute of Physics, The Hebrew University of Jerusalem, Jerusalem 91904, Israel
Received 2017 February 14; revised 2017 April 21; accepted 2017 April 23; published 2017 June 20

Abstract

We explore the implications of the low-spin components along the orbital axis observed in an Advanced LIGO O1 run on binary black hole (BBH) merger scenarios in which the merging BBHs have evolved from field binaries. The coalescence time determines the initial orbital separation of BBHs. This, in turn, determines whether the stars are synchronized before collapse, and hence determines their projected spins. Short coalescence times imply synchronization and large spins. Among known stellar objects, Wolf–Rayet (WR) stars seem to be the only progenitors consistent with the low aligned spins observed in LIGO's O1, provided that the orbital axis maintains its direction during the collapse. We calculate the spin distribution of BBH mergers in the local universe, and its redshift evolution for WR progenitors. Assuming that the BBH formation rate peaks around a redshift of ∼2–3, we show that BBH mergers in the local universe are dominated by low-spin events. The high-spin population starts to dominate at a redshift of ∼0.5–1.5. WR stars are also progenitors of long gamma-ray bursts that take place at a comparable rate to BBH mergers. We discuss the possible connection between the two phenomena. Additionally, we show that hypothetical Population III star progenitors are also possible. Although WR and Population III progenitors are consistent with the current data, both models predict a non-vanishing fraction of high positive values of the BBHs' aligned spin. If those are not detected within the coming LIGO/Virgo runs, it will be unlikely that the observed BBHs formed via field binaries.

Key words: black hole physics – gamma-ray burst: general – gravitational waves

1. Introduction

The Advanced LIGO gravitational-wave (GW) detectors discovered mergers of binary black holes (BBHs). (Abbott et al. 2016c). This discovery has created an opportunity for GW astronomy of black holes. The GW measurements using a matched filter analysis provide us valuable information on the GW sources, e.g., the masses and spins of the BBHs. In addition, the luminosity distance or the cosmological redshift of the sources can also be measured, and thus, the event rate of BBH mergers can be obtained. The resulting mass function of the primaries is consistent with the Salpeter initial mass function (Abbott et al. 2016b). Additionally, the inferred event rate is surprisingly high, about 0.1% of the current core-collapse supernova rate, suggesting that these are not the results of an obscure rare phenomenon. These facts motivate us to consider here the formation pathway of merging BBHs, as well as their binary evolution and impact on our understanding of astrophysical phenomena involving stellar mass black holes (see e.g., Abbott et al. 2016a and references therein).

The formation pathway of merging BBHs is one of the most intriguing mysteries that arose after the LIGO's discovery. One of the puzzles to solve is how such massive BBHs form in close binary systems. These massive stellar progenitors are expected to evolve to giant stars whose stellar radii significantly exceed the semimajor axis that allows BBHs to merge within a Hubble time.

One possible scenario involves a dynamically unstable common envelope phase (see e.g., Belczynski et al. 2016). Although many works have been dedicated to this issue (see, e.g., Kruckow et al. 2016 for a recent work and Ivanova et al. 2013 and references therein), the outcomes of common envelope phases remain unknown. Other scenarios that avoid common envelope phases include chemically homogeneous evolution (Mandel & de Mink 2016), rapid-mass transfers (van den Heuvel et al. 2017), massive overcontact binaries (Marchant et al. 2016), and Population (Pop) III progenitors (Kinugawa et al. 2014; Inayoshi et al. 2017). We consider these scenarios here. We do not discuss here other scenarios that are not based on binary stellar evolution: a dynamical capture in dense stellar clusters (O'Leary et al. 2016; Rodriguez et al. 2016a), formation in galactic nuclei (Antonini & Rasio 2016; Bartos et al. 2017; Stone et al. 2017), or primordial BBHs (Ioka et al. 1998; Bird et al. 2016; Blinnikov et al. 2016; Kashlinsky 2016; Sasaki et al. 2016).

One route to approach the progenitor scenario, on which we focus on in this paper, is to derive the required conditions for the progenitors of BBH mergers from the observed parameters of the systems. This method allows us to avoid numerous uncertainties in modeling of the stellar evolution and the binary interaction. Kushnir et al. (2016) have recently pointed out that, among their observable quantities, the spin of merging BBHs parallel to the orbital axis seems to be the most useful in constraining the progenitor properties (see also Zaldarriaga et al. 2017). They have shown that the coalescence time of GW150914 is longer than 1 Gyr, if this merger arose from Wolf–Rayet (WR) stars in a field binary system. These discussions assume that natal kicks during the collapse do not significantly change the orbital angular momentum such that the aligned spin parameters are expected to have positive values. It is worth noting that the aligned spin parameters measured by LIGO can be negative. Such negative values are naturally expected in the dynamical capture scenario and cosmological scenario (Bird et al. 2016; Blinnikov et al. 2016; Rodriguez et al. 2016b).

The event rate of BBH mergers inferred by the LIGO's detections is similar to the rate of long Gamma-Ray Bursts (LGRBs) after beaming correction with a reasonable value

Table 1
Parameters of the BBH Mergers Detected During LIGO's O1 Run

Event	m_1 ($M_\odot$)	m_2 ($M_\odot$)	$m_{\rm tot}$ ($M_\odot$)	$\chi_{\rm eff}$	Rate (Gpc^{-3} yr^{-1})
GW150914	$36.2^{+5.2}_{-3.8}$	$29.1^{+3.7}_{-4.4}$	$65.3^{+4.1}_{-3.4}$	$-0.06^{+0.14}_{-0.14}$	$3.4^{+8.6}_{-2.8}$
GW151226	$14.2^{+8.3}_{-3.7}$	$7.5^{+2.3}_{-2.3}$	$21.8^{+5.9}_{-1.7}$	$0.21^{+0.20}_{-0.10}$	37^{+92}_{-31}
LVT151012	23^{+18}_{-6}	13^{+4}_{-5}	37^{+13}_{-4}	$0.0^{+0.3}_{-0.2}$	$9.4^{+30.4}_{-8.7}$

Note. The parameters are median values with 90% confidence intervals. These values are taken from Abbott et al. (2016b).

(Wanderman & Piran 2010). LGRBs are produced during the core collapse of massive stars. They are believed to form from a black hole surrounded by an accretion disk (Woosley 1993), which requires rapid rotation of the progenitor. These facts motivate us to explore the possibility that LGRBs are produced during the core collapse of massive stars in close binaries that eventually evolve to merging BBHs. In fact, such scenarios in which LGRBs arise from massive stars in close binaries have been already discussed (e.g., Podsiadlowski et al. 2004; Detmers et al. 2008; Woosley & Heger 2012).

In this paper, we consider the spins of BBH mergers for different types of progenitors and estimate the expected spin distribution and its redshift distribution. We briefly summarize the observed aligned spins of the BBH mergers detected in LIGO's O1 run in Section 2. We describe the spin and tidal synchronization of the progenitors in Sections 3 and 4, and discuss different stellar models in Section 5. The possible connection between the BBH merger progenitors and LGRBs is discussed in Section 6. We show the spin distribution and its redshift evolution for the case of WR progenitors and Pop III progenitors in Section 7. We also discuss caveats of the spin argument in Section 8. We conclude our results in Section 9. In this paper, we use a ΛCDM cosmology, with $h = 0.7$, $\Omega_\Lambda = 0.7$, and $\Omega_M = 0.3$.

2. LIGO's O1 GW Detections

Mass function and rate: The masses and event rates of the three BBHs detected in LIGO's O1 run are summarized in Table 1. These event rates suggest that the primary mass function of BBH mergers is $dR/dm_1 \propto m_1^{-\alpha}$, where $\alpha = 2.5^{+1.5}_{-1.6}$ and m_1 is the mass of the primaries. The total BBH merger rate density is then 99^{+138}_{-70} Gpc^{-3} yr^{-1} for $\alpha = 2.35$ and $m_{1,\rm min} = 5\,M_\odot$, where this minimal mass is based on the observed population of these mergers (Abbott et al. 2016b). This choice is consistent with observations of Galactic black holes (see, e.g., Özel et al. 2010; Farr et al. 2011). Note that the total event rate is sensitive to the choice of $m_{1,\rm min}$, which is still uncertain. If we take the secondary mass of GW151226, 7.5 $M_\odot$, as the minimal black hole mass in BBH mergers, then the total event rate decreases to 57 Gpc^{-3} yr^{-1}.

This primary mass function is consistent with the Salpeter initial mass function of local stars (Abbott et al. 2016b), suggesting that these BBHs may originate from binary stellar objects. In addition, the event rate is similar to that of LGRBs, which are thought to be associated with black hole formations. In Sections 7 and 8, we will discuss a scenario motivated by this similarity, in which LGRBs are produced at the core collapse of massive stars in binary systems that eventually evolve to BBH mergers.

Spin parameters: The spin angular momentum of the merging BBHs can be inferred from the GW signals. The effective spin parameter $\chi_{\rm eff}$ is a mass-weighted mean spin angular momentum of the two black holes parallel to the orbital angular momentum:

$$\chi_{\rm eff} \equiv \frac{m_1}{m_{\rm tot}}(\boldsymbol{s}_1 \cdot \hat{L}) + \frac{m_2}{m_{\rm tot}}(\boldsymbol{s}_2 \cdot \hat{L}), \quad (1)$$

where m_2 is the secondary mass, $m_{\rm tot} = m_1 + m_2$, $\boldsymbol{s}_1$ and $\boldsymbol{s}_2$ are the specific spin angular momenta of the primary and secondary normalized by the speed of light c, gravitational constant G, and mass of each component, and $\hat{L}$ is the unit vector of the orbital angular momentum. This is well-constrained as compared with the individual component spins, which are not. The measured values are shown in Table 1. The parameter region of $\chi_{\rm eff}$ is $-1 \leqslant \chi_{\rm eff} \leqslant 1$, where the lower limit arises when both black holes' spins are maximal and anti-aligned to the orbital axis, and the upper limit when both are maximal and aligned. If one of the black holes' spins is maximal and aligned and the other one is not, we expect $\chi_{\rm eff} \approx 0.5$ for equal mass BBHs. The observed values of $\chi_{\rm eff}$ clearly exclude rapidly rotating synchronized progenitors whose spin axis is parallel to the orbital axis. As pointed out by Kushnir et al. (2016) and Rodriguez et al. (2016b), these measured effective spin parameters depend sensitively on the evolutionary path of progenitors of BBHs and provide important constraints on the origin of BBH mergers. We focus on the spin evolution of the BBH progenitors in the rest of the paper. Note that the error range of the observed $\chi_{\rm eff}$ of GW151226 does not exclude the possibility that the spin parameter of the secondary is on the order of unity if the primary's spin is much smaller than unity.

3. BBH Progenitors' Spin

A binary system with stellar masses m_1 and m_2 at a semimajor axis a in-spirals, due to GW radiation. The time until the coalescence, t_c, is (Peters 1964):

$$t_c = \frac{5}{256}\frac{a}{c}\frac{c^2 a}{G m_1}\frac{c^2 a}{G m_2}\frac{c^2 a}{G m_{\rm tot}} \approx 10 q^2 \left(\frac{2}{1+q}\right)\left(\frac{a}{44 R_\odot}\right)^4\left(\frac{m_2}{30\,M_\odot}\right)^{-3} {\rm Gyr}, \quad (2)$$

where $q \equiv m_2/m_1$. For binaries with $t_c = 10$ Gyr, the corresponding orbital period is: $P_{\rm orb} \approx 4.4$ day $(a/44\,R_\odot)^{2/3}$ $(m_{\rm tot}/60\,M_\odot)^{-1/2}$. Note that, for simplicity, we assume circular orbits here and elsewhere. Such orbits are expected within most binary evolution scenarios (see, e.g., Zahn 1977 for the orbital circularization due to the tidal torque), as long as natal kicks at the black hole formation are not significant.

The stellar radius cannot exceed the Roche limit. The Roche limit of the secondary (Eggleton 1983) is $R_{\rm RL} \approx 0.49 q^{2/3} a/[0.6q^{2/3} + \ln(1+q^{1/3})]$. For equal mass binaries, $R_{\rm RL} \approx 0.38a$. We denote hereafter the primary (secondary) as the first (second) star evolving to core collapse. Requiring $R_2 < R_{\rm RL}$ and a coalescence time less than a Hubble time yields:

$$R_2 \lesssim 17\, R_\odot (m_2/30\, M_\odot)^{3/4}, \tag{3}$$

where R_2 is the stellar radius of the secondary and we have assumed $q = 1$. In the rest of this paper, we consider massive stars that satisfy this condition.

Clearly, if the stellar spin just before the collapse is larger than the maximal Kerr black hole spin, some mass and angular momentum will be shed out and the formed black hole will be a maximal Kerr. Otherwise, the spin angular momentum of the black hole equals its progenitor's (see, e.g., Barkov & Komissarov 2010, and also Sekiguchi & Shibata 2011; O'Connor & Ott 2011 for numerical studies). A critical question is whether the star is synchronized (tidally locked) with the orbital motion before the collapse. We characterize this with a synchronization parameter x_s; e.g., $x_s = 1$ and 0 correspond to a star tidally synchronized with the orbital motion and a non-rotating star, respectively. We do not expect negative values of x_s (counter rotating stars) and values larger than unity.

If there are no significant mass and angular momentum losses from the system during the collapse the spin of the secondary black hole is characterized by its stellar mass, radius, and semimajor axis:

$$J_2 = x_s I_2 \Omega_{\rm orb}, = x_s \epsilon m_2 R_2^2 \left(\frac{G m_{\rm tot}}{a^3}\right)^{1/2}, \tag{4}$$

where ϵ characterizes the star's moment of inertia $I_2 \equiv \epsilon m_2 R_2^2$. Here and in the following, we consider, for simplicity, rigidly rotating stars. The spin parameter is then

$$\begin{aligned}\chi_2 &\equiv \frac{J_2}{m_2 r_{g,2} c}, \\ &= x_s \epsilon \left(\frac{R_2}{r_{g,2}}\right)^{1/2}\left(\frac{R_2}{a}\right)^{3/2}\left(\frac{m_{\rm tot}}{m_2}\right)^{1/2} \approx x_s \left(\frac{\epsilon}{0.075}\right) \\ &\times \left(\frac{R_2}{4.7\, R_\odot}\right)^{2}\left(\frac{a}{44\, R_\odot}\right)^{-3/2}\left(\frac{m_{\rm tot}}{2m_2}\right)^{1/2}\left(\frac{m_2}{30\, M_\odot}\right)^{-1/2},\end{aligned} \tag{5}$$

where $r_{g,2} \equiv G m_2/c^2$. The normalizations of R_2 and a were chosen such that the spin parameter is unity for $x_s = 1$ and the merger takes place on a timescale of 10 Gyr.

The spin parameter can be directly related to the merger timescale:

$$\begin{aligned}\chi_2 \approx x_s\, q^{1/4}&\left(\frac{1+q}{2}\right)^{1/8}\left(\frac{\epsilon}{0.075}\right) \\ &\times \left(\frac{t_c}{10\ {\rm Gyr}}\right)^{-3/8}\left(\frac{R_2}{4.7\, R_\odot}\right)^{2}\left(\frac{m_2}{30\, M_\odot}\right)^{-13/8}.\end{aligned} \tag{6}$$

4. Synchronization

In close binary systems, the tidal torque on the stars forces them to reach an equilibrium state, where the stellar rotation is synchronized with the orbital motion. The synchronization timescale of a star with a radiative envelope and a convective core can be estimated as

$$\begin{aligned}t_{\rm syn} \approx 0.07\ {\rm Myr}\, q^{-2}&\left(\frac{1+q}{2}\right)^{-5/6}\left(\frac{\epsilon}{0.075}\right)\left(\frac{R}{14\, R_\odot}\right)^{-7} \\ &\times \left(\frac{M}{30\, M_\odot}\right)^{-1/2}\left(\frac{a}{44\, R_\odot}\right)^{17/2}\left(\frac{E_2}{10^{-6}}\right)^{-1},\end{aligned} \tag{7}$$

where E_2 is a dimensionless quantity depending on the stellar structure introduced by Zahn (1975). For massive, main sequence stars and WR stars, E_2 is $\sim 10^{-7}$–10^{-4} (Zahn 1975; Kushnir et al. 2017). It may be smaller for blue supergiants. For WR progenitors, Kushnir et al. (2016) derive a useful form of Equation (7) as:

$$t_{\rm syn} \approx 10\ {\rm Myr}\, q^{-1/8}\left(\frac{1+q}{2q}\right)^{31/24}\left(\frac{t_c}{1\ {\rm Gyr}}\right)^{17/8}. \tag{8}$$

We will use this form for WR progenitors in Section 7.

If the synchronization time is much shorter than other timescales, e.g., the stellar lifetime and the wind angular-momentum loss timescale, the star is synchronized with the orbital motion, i.e., $x_s = 1$. On the other hand, if the synchronization time is much longer than the others, the stellar spin parameter decreases with time, due to the wind loss from the initial value.

If the synchronization timescale is comparable to the stellar lifetime or the wind timescale, which is the case for WR progenitors, one needs to solve the time evolution of the synchronization parameter. In the following, we estimate the spin evolution of close binary WR stars using the formulation of Kushnir et al. (2016), which takes into account the tidal synchronization, wind mass loss, and stellar lifetime. Given an initial value $x_{s,i}$ at the beginning of the WR phase, the synchronization parameter evolves as:

$$\frac{dx_s}{d\tau} = \frac{t_w}{t_{\rm syn}}(1 - x_s)^{8/3} - x_s, \tag{9}$$

where t_w is the timescale of spin angular momentum loss and $\tau = t/t_w$. The solution approaches to an equilibrium value, $x_{s,\rm eq}$, at late times:

$$\frac{t_w}{t_{\rm syn}}(1 - x_{s,\rm eq})^{8/3} = x_{s,\rm eq}. \tag{10}$$

Note, however, that t cannot exceed the stellar lifetime t_*. The approximate solutions at t_* are summarized in Kushnir et al. (2016), for different parameter regions.

If the timescale of the angular momentum loss due to the wind is longer than the stellar lifetime, the synchronization parameter of a star at the end of its lifetime, $x_{s,f}$, can be estimated as:

$$x_{s,f} \approx \begin{cases} \max(1 - t_*/t_w,\ x_{s,\rm eq}) & \text{for } x_{s,i} = 1, \\ \min(t_w/t_{\rm syn},\ x_{s,\rm eq}) & \text{for } x_{s,i} = 0. \end{cases} \tag{11}$$

In order to estimate the synchronization parameter of the WR stars at the end of their life in Section 7, we will use the

above solutions with the following parameters: $t_w = 1$ Myr and $t_{\rm WR} = 0.3$ Myr (Langer et al. 1994; Meynet & Maeder 2003, 2005). Using the synchronization parameter, we calculate the spin parameter of the individual black holes for a given mass, radius, and coalescence time t_c.

For the wind angular momentum losses, we assume that isotropic winds remove the outermost spherical shell of a star with spin angular momentum of $2M_s R_*^2 \Omega_*/3$, where M_s is the mass of the shell, and R_* and Ω_* are the stellar radius and spin angular frequency. In this description, $t_w \approx 1$ Myr corresponds to a mass loss rate of $\sim 10^{-5.5}\, M_\odot\ {\rm yr}^{-1}$. Note that, however, the efficiency of the spin angular momentum loss due to winds can be either lower or higher. For instance, winds may have anisotropic structures, due to a fast stellar rotation, that remove less spin angular momentum (Meynet & Maeder 2007). On the other hand magnetic winds carry out spin angular momentum more efficiently, depending on the field strength (e.g., Ud-Doula et al. 2009). Note also that a significant mass loss from a binary increases the semimajor axis. However, because the spin angular momentum is more efficiently lost from the stellar surface for rigidly rotating stars, the mass-loss timescale is $\sim 10 t_w (0.075/\epsilon)$ for the isotropic winds. With the parameters we consider here, this effect on the semimajor axis is negligible.

The GW measurements are quite insensitive to the spin components perpendicular to the orbital axis, as the observed $\chi_{\rm eff}$ measures only the spin parallel to the orbital axis. In the following discussion, we assume that the misalignments of the BBHs' spin axes to the orbital axis are negligible, and hence the synchronization parameters cannot be negative. This assumption is valid as long as the progenitor binaries do not receive significant kicks at the black hole formation. As we will discuss in Section 8, such kicks are unlikely when black holes form. On the contrary, the dynamical capture scenario of merging BBH formation naturally predicts that half of these mergers have negative values of $\chi_{\rm eff}$. Note that the measured effective spin parameters of GW150914 and LVT151012 allow negative values within errors. Therefore, the discovery of BBHs with a negative $\chi_{\rm eff}$ will have a significant impact on the understanding of the formation scenarios and the kick at the black hole formation (Rodriguez et al. 2016b).

5. Synchronization for Different Stellar Models

As the stellar radius and resulting black hole's spin are tightly connected, the spin measurements strongly constrain the possible progenitors of the observed BBH mergers. Population synthesis calculations considering the stellar evolution and the binary interactions are often used to estimate the rate, mass, and spin distribution of compact binary mergers and to discuss their progenitors. Here, we take a different approach. We do not discuss the binary evolution; instead, we focus on the the observed low-aligned spins and examine their implications on the stellar progenitor just before its core collapse to a black hole.

We consider known types of massive stellar objects and hypothetical Pop III stars. The BBH mergers event rate suggests that, if they form via binary stellar evolution, there are $\sim$10 or less such progenitors in the Galaxy (using $0.01\ {\rm Mpc}^{-3}$ as the number density of Milky Way-sized galaxies, and a stellar lifetime of 1 Myr). With such a small number, it is possible and even likely that we have not identified these objects in the Galaxy. It is interesting to note, in passing, that *Gaia* might be able to identify these binaries, as they involve the most massive, and hence most luminous, stars.

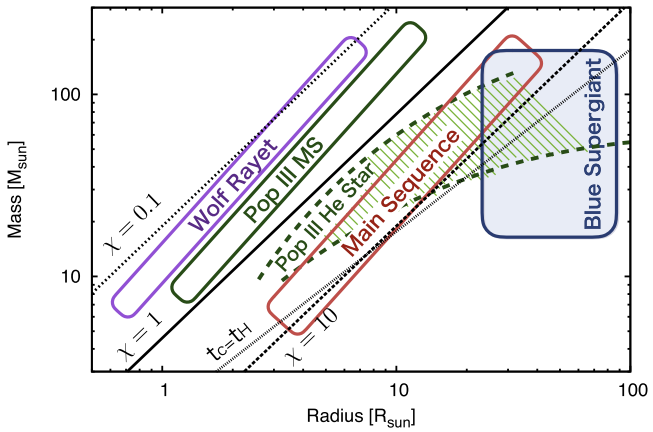

Figure 1. Mass–radius relations of different stellar models. The diagonal (dotted, solid, and short-dashed black) lines depict the resulting black hole dimensionless spin for these masses and radii, assuming that the star is synchronized at a semimajor axis where the coalescence time is a Hubble time. Also shown as a diagonal line labeled by $t_c = t_{\rm H}$ is the stellar radius limited by the Roche limit. Stars on the right side of this line cannot exist in a binary system whose coalescence time is less than a Hubble time. The curves are drawn for a mass ratio, q, of unity. One can clearly see that most models will result in χ values much larger than unity.

Figure 1 depicts the mass–radius relation of the different stellar models. Three diagonal lines depict the spin parameters of these stars $\chi = 0.1$, 1, and 10 (see Equation (5)), if they are synchronized at the semimajor axis for which a binary coalesces in a Hubble time. Also shown as a diagonal line is the critical stellar radius that exceeds the Roche limit in a binary system that coalesces in a Hubble time (see Equation (3)). Figure 2 shows the relation between the effective spin parameters of different stellar models with the observed values from Abbott et al. (2016b). Here, we assume a mass ratio $q = 1$, the single (double) synchronization means that one (both) of the black holes in a BBH is formed from a synchronized star. When comparing the models with the measured values of $\chi_{\rm eff}$, we further assume that the spin axes of BBHs are aligned with the orbital axis (see Section 8 for caveats).

For a given stellar model and a given coalescence time, the spin parameter of the synchronized progenitors depends rather weakly on the stellar mass. More specifically, the spin parameter behaves as $\chi \propto m^{-0.225}$ for $R \propto m^{0.7}$, which is a typical dependence of the radius of massive stars on the mass (Tout et al. 1996; Kushnir et al. 2016). Thus, the spin parameter reflects the time delay between the formation and the coalescence irrespective of the BBH mass.

(i) Main-sequence stars: Although we do not expect a main-sequence star to collapse directly to a black hole, we begin with main-sequence binaries and show that these are ruled out. Main-sequence stars with masses $\gtrsim 10\, M_\odot$ can exist in a binary system with $t_c = 10$ Gyr without exceeding its Roche limit.

Massive main-sequence stars in close binaries with $t_c \lesssim 10$ Gyr are synchronized on timescales much shorter than their lifetime (see Equation (7), where we used the stellar structure of main-sequence stars at the median point of their lifetime; Tout et al. 1996; Hurley et al. 2000). Thus, main-sequence stars are tidally synchronized. In fact, Galactic O-star binaries with orbital periods $\lesssim$10 days are likely to be tidally synchronized (Ramírez-Agudelo et al. 2015). The spin

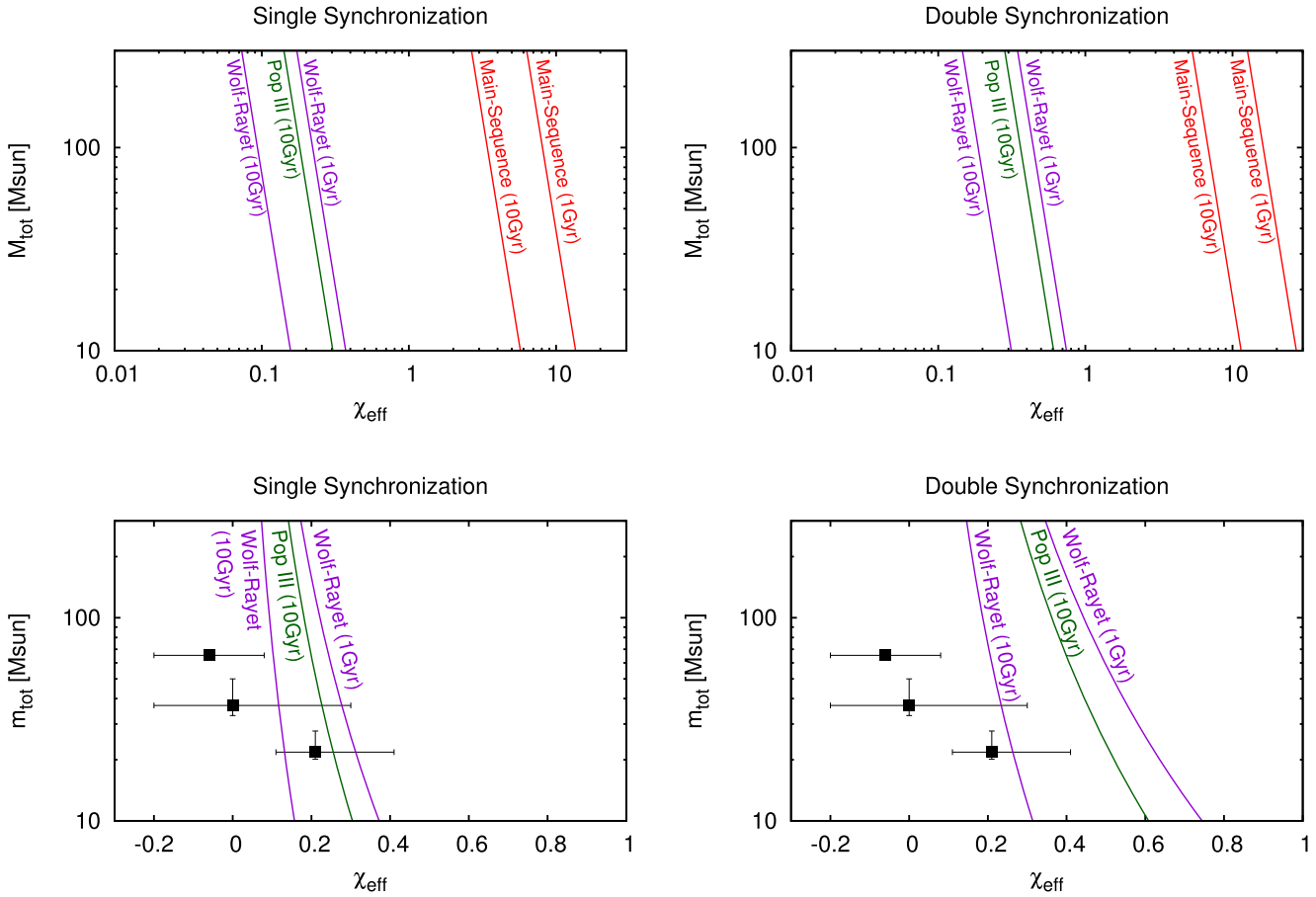

Figure 2. Spin and total mass of binaries in which the stellar rotation is synchronized with the orbital motion. Here, we consider different stellar models with coalescence times of 1 or 10 Gyr. The top panels show effective spin parameters in logarithmic scales. The bottom panel shows effective spin parameters ranging from −0.3 to 1. Here, we assume the the mass ratio of binaries is unity for the models. When comparing the models with the data in the bottom panels, we also assume that the BBH spin axes are aligned to the orbital axis. The data are taken from Abbott et al. (2016b).

parameter of such main-sequence stars always exceeds unity. Therefore, we can rule out the possibility that the BBHs detected in LIGO's O1 run have been formed directly from the collapse of main-sequence stars.

If the BBHs formed via binary evolution begin with two main-sequence stars, then in order to reduce the spin parameter significantly, the progenitors must have experienced either a significant mass loss that dispersed most of their spin angular momentum (more than 95%) or a significant decrease in the semimajor axis during their evolution. The former may occur due to a wind or to mass transfer during the late phase, and the latter may occur during a common envelope phase. The natural outcomes of these processes are WR stars, which we discuss later in this and the following sections. This conclusion seems to be consistent with stellar and binary evolution models (e.g., Belczynski et al. 2016).

(ii) Red supergiant stars are late massive stars with an extended hydrogen envelope, in which the convection is deeply developed. These stars are located around the Hayashi line in HR diagrams, where the corresponding temperatures are around 3000–4000 K. Red supergiants have high luminosities and cool effective temperatures, implying that they have large radii of 100–$10^3\,R_\odot$. BBHs arising from such wide binaries never merge within a Hubble time, so we can robustly exclude the scenario that red supergiants are the progenitors of merging BBHs just prior to the core collapse.

(iii) Blue-supergiant stars are massive stars in their late phase, with a hydrogen radiative envelope (see, e.g., Langer et al. 1994; Hirschi et al. 2004; Meynet et al. 2011). Their radii can be 10–30 $R_\odot$, corresponding to high effective temperatures, and can be smaller than the Roche limit of a binary with a coalescence time of 10 Gyr. The spin parameter of blue supergiants is always much larger than unity if they are synchronized. Therefore, these stars are unlikely to be progenitors of LIGO's O1 events. However, the synchronization time is quite sensitive to the structure of the envelope, and hence it is somewhat uncertain. We will address this issue in a separate work.

(iv) WR stars are late-phase massive stars that have lost most of their hydrogen envelope (see, e.g., Langer et al. 1994; Meynet & Maeder 2003, 2005). Importantly, a few WR–black hole binaries that are likely to evolve to merging BBHs have been observed in nearby galaxies (see Prestwich et al. 2007 and Silverman & Filippenko 2008 for IC10 X-1; Carpano et al. 2007 and Crowther et al. 2010 for NGC 300 X-1; Bulik et al. 2011 for the inferred BBH merger rate; Liu et al. 2013 for M 101 ULX-1; see also Esposito et al. 2015 for more candidates). Because of the lack of a hydrogen envelope, the stellar radius is small. It is related to the mass as $R \approx R_\odot (M/10\,M_\odot)^{0.7}$ (Kushnir et al. 2016). The spin parameters of BBHs formed via synchronized WR stars are shown in Figure 2. For systems with $t_c \sim 10$ Gyr, the spin parameters can be as small as 0.1. These values are consistent with the

measured effective spin parameters of the LIGO's O1 events. However, based on Equation (8), WR stars are so compact that WR stars in binaries with $t_c \gtrsim 1$ Gyr are not tidally synchronized within their lifetime. We will discuss further the spin parameters of WR progenitors in Section 7.

(v) Population III stars have formed from pristine gas. They are typically massive stars, with twenty to a few hundred $M_\odot$ (Hosokawa et al. 2011; Hirano et al. 2014). Their radii are much smaller than those of normal main-sequence stars because the core, which lacks metals, needs to be compact in order to produce sufficient heat through nuclear burning to support the stellar mass (e.g., Omukai & Palla 2003). Because Pop III stars form only in the very early universe, around a redshift of ∼10 (e.g., de Souza et al. 2011), BBH mergers at the local universe that originate from Pop III stars have a coalescence time of ∼10 Gyr. Using the Pop III stellar structure calculated by Marigo et al. (2001), we find that, even though Pop III stars are small, if they are synchronized, the spin parameters of BBH mergers in the local universe are between 0.2 and 0.6 (see Figure 4). However, the synchronization time of such systems is ∼10 Myr, which is comparable to their lifetime, so that Pop III stars in such binaries may not be fully synchronized. Therefore, Pop III stars can be the progenitors of LIGO's O1 events.

The spin parameter of Pop III stars exceeds unity if the synchronization occurs during the He-burning phase (see Figure 1). However, these stars have a convective core with a small radius and a shorter lifetime, therefore synchronization probably does not occur during this Pop III He burning phase. Furthermore, massive Pop III He stars exceed their Roche limit (see Figure 1). Therefore, some fraction of the spin angular momentum may be removed due to mass transfer in this phase.

6. Long GRBs and BBH Mergers

LGRBs arise from the core collapse of massive stars. Supernovae associated with LGRBs are type Ibc, suggesting that the progenitors are stripped stars, e.g., WR stars. The progenitors' radii can be estimated from the properties of the prompt emissions as follows. The plateau in $dN_{\rm GRB}/dT_{90}$ (where $N_{\rm GRB}$ is the number of observed LGRBs, and T_{90} is the duration of prompt emission containing 90% of its gamma-ray fluence) indicates that the typical jet break-out time from the stellar surface is ∼15 s (Bromberg et al. 2012). This break-out time is related to the progenitor's parameters as (Bromberg et al. 2011):

$$t_b \approx 15\ {\rm s}\left(\frac{L_{j,{\rm iso}}}{10^{51}\ {\rm erg\ s^{-1}}}\right)^{-1/3}\left(\frac{\theta_j}{10^\circ}\right)^{2/3} \times \left(\frac{R_*}{5\,R_\odot}\right)^{2/3}\left(\frac{M_*}{15\,M_\odot}\right)^{1/3}, \quad (12)$$

where $L_{j,{\rm iso}}$ is the isotropic jet luminosity, θ_j is the jet's half opening angle, and R_* and M_* are the radius and mass of the progenitor. Note that the mass and radius that are inferred from the GRB observations of $L_{j,{\rm iso}}$, θ_j, and t_b are consistent with the required properties of the progenitors of BBH mergers.

The spin of the progenitor likely plays an essential role in the production of the GRB emission because the formation of a massive accretion torus around a new-born black hole is required to produce the corresponding high luminosity jets (see, e.g., MacFadyen & Woosley 1999). The specific orbital angular momentum at the inner most stable circular orbit is $j_{\rm ISCO} = 2\sqrt{3}$ for Schwarzschild black holes, and $2/\sqrt{3}$ for extreme Kerr black holes. Here, the angular momentum is normalized by the mass of the central black hole. The specific angular momentum of a mass element of a rigidly rotating star at a radius R on the equatorial plane is

$$j(R) = \frac{\Omega R^2}{r_{g,{\rm BH}}\,c} = \frac{\chi_*}{\epsilon}\left(\frac{R}{R_*}\right)^2\left(\frac{M_*}{M_{\rm BH}}\right), \quad (13)$$

where $r_{g,{\rm BH}}$ is the gravitational radius of the central black hole and χ_* is the dimensionless spin parameter of the star. The condition that the mass elements of the stellar core form an accretion torus is assumed to be $j(R_c) \geqslant j_{\rm ISCO}$ or equivalently:

$$\chi_* \gtrsim 1.3\left(\frac{\epsilon}{0.075}\right)\left(\frac{R_c}{0.57\,R_\odot}\right)^{-2} \times \left(\frac{R_*}{1.6\,R_\odot}\right)^2\left(\frac{M_{\rm BH}}{15\,M_\odot}\right)\left(\frac{M_*}{20\,M_\odot}\right)^{-1}, \quad (14)$$

where we assume that the central black hole is a Schwarzschild black hole as a conservative choice and R_c is the stellar core radius.[3] The reference parameters are for a WR star taken from Kushnir et al. (2016). Within this model, LGRBs are produced by black holes only when the progenitor's spin parameter is larger than ∼1.3, and thus the resulting black hole has a large spin (see also Barkov & Komissarov 2010). Using Equation (6), this condition can be translated to the coalescence time for a given stellar mass as $t_c \lesssim 0.2$ Gyr $(m/30\,M_\odot)^{-13/8}$. Therefore, if the delay-time distribution is roughly $1/t$ and the minimal coalescence time is ∼10 Myr, one third of BBH formations with $t_c < 10$ Gyr have spins which may be large enough to produce LGRBs (see Section 7 for the delay-time distribution). Note that two LGRBs may lead to a single BBH merger, as both the first and the second core collapses may produce GRBs if they arise from a doubly synchronized system.

7. The Spin Distribution and its Redshift Evolution of BBH Mergers

We turn now to the redshift-dependent spin distribution of BBH mergers for different assumptions on the formation rate. We focus on WR progenitors. Here, we assume that the spin parameter is $\chi_{\rm BH} = \min(\chi_*, 1)$. We consider two different scenarios: (i) the WR stars are synchronized at the beginning of the WR phase, $x_{s,i} = 1$; (ii) the initial spins of the WR stars are much smaller than the synchronization spin, $x_{s,i} \approx 0$. This latter, initially low spin case, $x_{s,i} = 0$, corresponds to an evolutionary path with a common envelope phase in which the semimajor axis shrikes significantly just prior to the beginning of the WR phase. The spin distribution of BBH mergers can therefore be used to constrain whether or not a common envelope phase plays an important role for the BBH progenitors.

The BBH merger rate at a given redshift is given by a convolution of the cosmic BBH formation rate and the

[3] If we use as the condition of the disk formation that the mass elements of the core surface have the specific angular momentum of the marginally bound orbit, which is four for a Schwarzschild black hole (as chosen in Barkov & Komissarov (2010)), the critical stellar spin parameter is larger by 15%, compared to Equation (14).

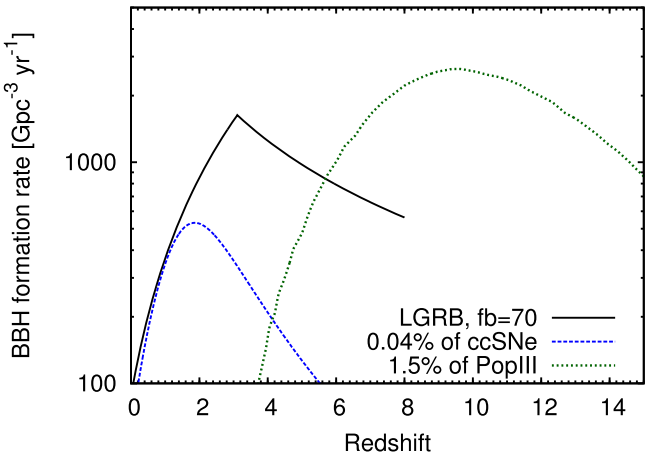

Figure 3. BBH formation rate, under the assumptions that it follows (i) the cosmic star formation history, (ii) the LGRB rate, and (iii) the Pop III star formation rate. The BBH formation rate is normalized to be 0.04% of core collapse supernovae for (i; Madau & Dickinson 2014), the LGRB rate with a beaming correction of 70 for (ii; Wanderman & Piran 2010), and 1.5% of Pop III star formation for (iii; de Souza et al. 2011). Here, the mean stellar mass of Pop III stars is assumed to be 20 $M_\odot$.

delay-time distribution. Here, we assume a power law distribution of the delay time with a minimal delay time[4]:

$$\frac{dN}{dt_c} = \frac{N_0}{t_c^n} \quad (\text{for } t_c > t_{c,\min}), \tag{15}$$

where the normalization constant N_0 ensures that the integration of Equation (15) from $t_{c,\min}$ to a Hubble time is unity. We consider here $n = 1$ or 2 and $t_{c,\min} = 10$ Myr. Note that this kind of delay-time distribution is inspired by those of other astrophysical phenomena related to binary mergers. For instance, the delay-time distribution of type Ia supernovae has $n \approx 1$ and $t_{c,\min}$ of 40 Myr to a few hundreds of Myr (Maoz et al. 2014 and references therein), and that of short GRBs has $n \approx 1$ and $t_{c,\min} \approx 20$ Myr (Wanderman & Piran 2010; Ghirlanda et al. 2016).

For the cosmic BBH formation rate, we consider two scenarios: (i) it is proportional to the cosmic star-formation rate (SFR; Madau & Dickinson 2014) and (ii) it equals the LGRBs (Wanderman & Piran 2010). The normalization of the cosmic BBH formation of the LGRB scenario corresponds to the LGRB rate, corrected by a beaming factor of $f_b = 70$. For the cosmic SFR scenario, our normalization corresponds to one BBH formed every $2.5 \cdot 10^5\, M_\odot$ stellar mass formation. This roughly corresponds to a merging BBH formation rate that is 0.04% of the normal core-collapse supernova rate (assuming that one core collapse supernova occurs every 100 $M_\odot$ stellar mass formation formation). The cosmic BBH formation rates of these scenarios are shown in Figure 3.

7.1. The Spin Distribution of BBH Mergers in the Local Universe

Figure 4 depicts the spin distribution of merging BBHs at $z = 0.1$. For simplicity, we consider equal mass binaries. Also shown are the values and upper limits of the spin parameters χ_2 inferred from LIGO's O1 detections, assuming that the spin axes of BBHs are aligned with the orbital axis. We consider two cases relating the effective spin parameters to the component spin χ_2: (i) a single synchronization, where the primary[5] black hole's spin is negligibly small, i.e., $\chi_2 \approx 2\chi_{\rm eff}$; and (ii) a double synchronization, where the primary black hole is also synchronized with a comparable spin parameter. In this case, $\chi_2 \approx \chi_{\rm eff}$.

The spin distribution for $n = 1$ has two peaks. One is at a high spin $\chi_2 \sim 1$ and the other is at a low spin $\chi_2 \sim 0.15$ ($\ll 0.1$) for $x_{s,i} = 1$ (for $x_{s,i} = 0$). The latter low-spin peak corresponds to the spin parameter of BBHs that are formed at the cosmic BBH formation peak. The population is flat between the two peaks. This is simply because of $dN/d\ln\chi_2 \propto dN/d\ln t_c = \text{const}$, inferred from Equation (6). For $n = 2$, the population at higher spins ($\chi_2 \gtrsim 0.3$) dominates, as expected from the fact that there are more BBHs with shorter coalescence times, as $dN/d\ln\chi_2 \propto \chi_2^{8/3}$ for $\chi_2 \gtrsim 0.2$. This feature is irrespective of assumptions about the initial synchronization parameters and the cosmic BBH formation history. It suggests that a steep delay-time distribution with $n \gtrsim 2$ is inconsistent with the observed spin distribution. Clearly, given the different assumption, the spin parameter distribution should be between the single synchronization with $x_{s,i} = 0$ and the double synchronization with $x_{s,i} = 1$.

The bimodal spin distribution that we find is qualitatively similar to one found by Zaldarriaga et al. (2017). However, the peak at the high spin in our calculation is lower than that of Zaldarriaga et al. (2017). This is because we use a BBH formation history that peaks at a redshift of 2–3, such that the merger events in the local universe are dominated by a population with longer coalescence times, and therefore they have smaller spins.

7.2. The Redshift Evolution of High/Low Spin BBH Mergers

Figure 5 shows the redshift evolution of the BBH merger rate for the cosmic SFR and the LGRB scenarios. We divide the BBH mergers into two classes: (i) high spin ($\chi_2 > 0.3$) and (ii) low spin ($\chi_2 < 0.3$). This threshold spin value corresponds to coalescence times of 0.3 and 1.5 Gyr for $x_{s,i} = 0$ and $x_{s,i} = 1$, respectively. Because of the longer delay of the lower-spin population, the high-spin BBH mergers predominately occur at higher redshifts. In all cases, the merger rate of the low-spin population is larger than that of the high-spin one in the local universe. Another interesting feature is that the merger rate of the high-spin population starts to dominate over the low-spin one at a redshift of ~0.5–1.5. Mergers at such redshifts could be detected by upgraded GW detectors in future.

The BBH merger history, which is a convolution of the formation history with a delay-time distribution, is not very sensitive to the assumption of the BBH formation history, i.e., LGRB or cosmic star-formation history, as long as the latter peaks around a redshift of 2–3.

To produce LGRBs, the black holes should have extreme spins (see Section 6). This is not the case for LIGO's O1 detections.[6] However, as noted earlier, BBHs with high spins have short merger times; therefore, we do not observe most of these mergers in the local universe. If the delay-time

[4] The strong dependence of the merging time on the semimajor axis suggests such a distribution with $n \lesssim 1$.

[5] The primary black hole is the one formed at the first core collapse for our definition. It is not necessarily the more massive one.

[6] Unless the spin–orbit misalignments are significant. Note also that the observed $\chi_{\rm eff}$ of GW151226 does not rule out the possibility that the less-massive black hole has a spin parameter on the order of unity.

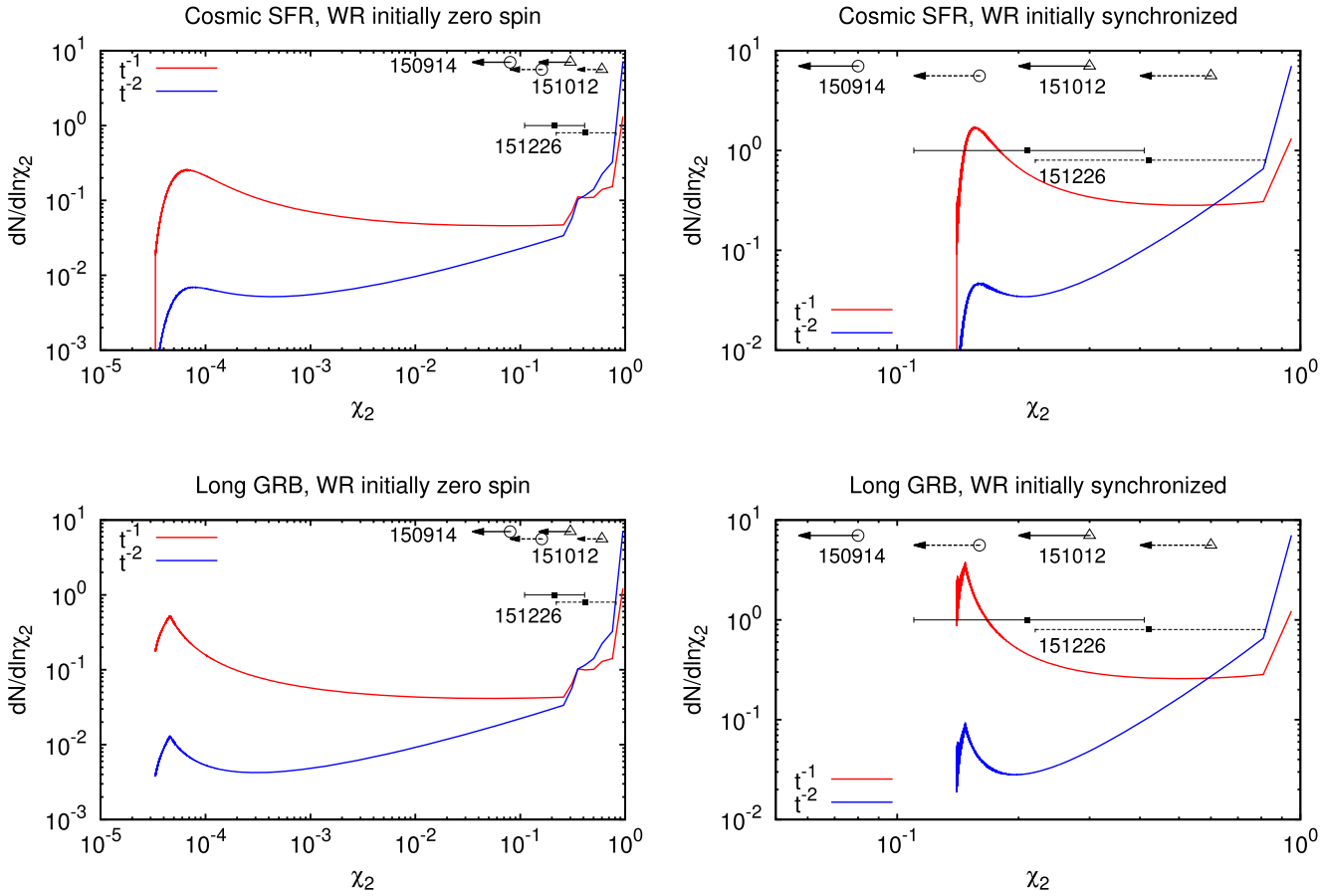

Figure 4. Spin distribution of BBH mergers at $z = 0.1$ for a BBH formation history that follows the cosmic star formation history (top panels) and the LGRB rate (bottom panels). The distributions are calculated under the assumptions that the initial spin angular momentum of the WR stars vanishes, i.e., $x_{s,i} = 0$ (left) and the WR stars are initially tidally synchronized, i.e., $x_{s,i} = 1$ (right). We use two different delay-time distributions, $n = 1$ and 2, with a minimal time delay of 10 Myr. We set the mass ratio, q, to be unity and the total mass to be 60 $M_\odot$. The location of the peak at lower spins slightly shifts with changing the masses. Also shown are the χ_2 values inferred from the LIGO's O1 three detections. The measured effective spin parameters are translated to χ_2 assuming $\chi_1 = \chi_2$ (solid line and arrows) and $\chi_1 = 0$. Here, we assume that the BBH spin axes are aligned with the orbital axis; hence, we show the upper limits on the spin parameters of GW150914 and LVT151004. Note that the measured spin parameters of these BBHs can be negative (see Table 1).

distribution is $\sim 1/t$, with $t_{\rm min} = 10$ Myr, we expect that the current event rate of BBH mergers with extreme spins is $\leqslant 20\%$ of the total merger rate. The corresponding high-spin BBH merger rate is $\lesssim 20^{+28}_{-14}$ Gpc^{-3} yr^{-1}. On the other hand, the local rate of LGRBs is $\sim 91^{+42}_{-49}$ Gpr^{-3} yr^{-1}($f_b/70$), where f_b is a beaming correction factor (Wanderman & Piran 2010). Note that the LGRB rate should be compared with double the high-spin BBH merger rate for the double synchronization case. These rates are consistent with each other, within the admittedly large uncertainties. This suggests that it is possible that the two phenomena share same progenitors.

7.3. Pop III BBH Mergers

Figure 6 shows the redshift evolution of BBH mergers for the Pop III scenario. Here, we use a Pop III SFR derived by de Souza et al. (2011).[7] We normalize the Pop III BBH formation rate such that 1.5% of Population III stars form BBHs with coalescence times less than a Hubble time (Inayoshi et al. 2017). Here, we assume a mean stellar mass of 20 $M_\odot$, a delay-time distribution with $n = 1$, and a minimal time delay of 0.4 Gyr. This minimal time delay roughly corresponds to the minimal semimajor axis for which the radius of Pop III main-sequence stars is smaller than the Roche limit.

The redshift evolution of Pop III BBH mergers is significantly different from other astrophysical scenarios. It increases up to $z \sim 5$, which is beyond the peaks of the cosmic star-formation history and the LGRB rate. This by itself can be used to distinguish this scenario from the others (see also Nakamura et al. 2016). Another prediction of this scenario is that the spin parameters of BBH mergers at higher redshifts above ~4–5 may be dominated by an extreme spin population with $\chi_2 \sim 1$. Clearly, significant improvements in GW detectors is needed to detect such events.

8. Caveats

Uncertainties in the synchronization: The tidal synchronization relevant to the BBH progenitors is due to dynamical tides that are excited above the convective core and dissipate in the radiative envelope (Zahn 1975; Goldreich & Nicholson 1989; Kushnir et al. 2017). Once a stellar structure is given, one can calculate the tidal torque on the star. However, massive stellar envelopes might be turbulent and unstable. In such cases, synchronization due to an equilibrium tide in the envelope can be more efficient (see, e.g., Toledano et al. 2007;

[7] This Pop III star-formation rate seems to be the maximum allowed by the Planck observations of the electron-scattering opacity of the cosmic microwave background, within two σ (see, e.g., Visbal et al. 2015 for details).

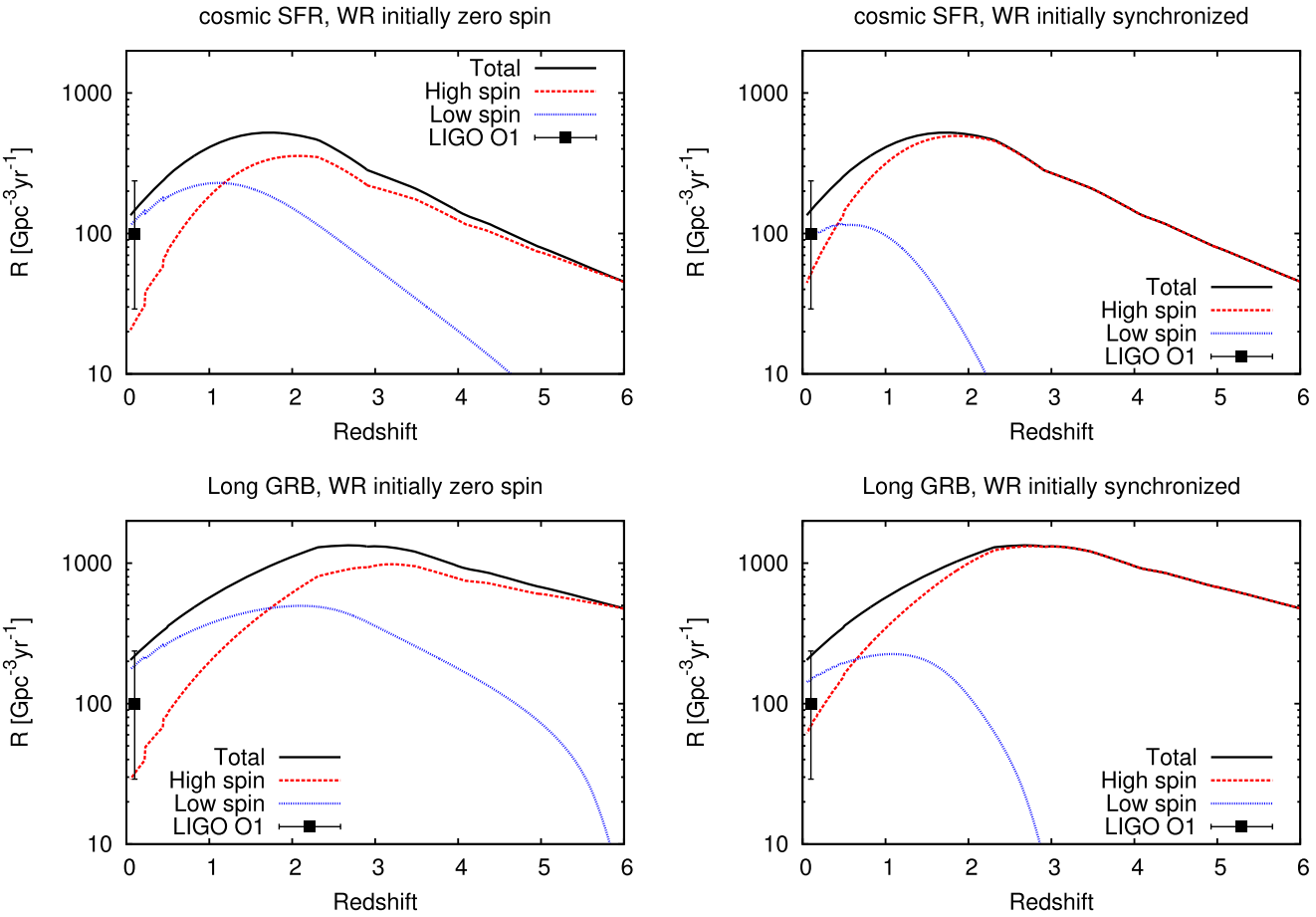

Figure 5. Redshift evolution of BBH mergers for the cases where BBH formation follows the cosmic star-formation history (top panels) and the LGRB rate (bottom panels). We separate the mergers into the high- and low-spin populations, with a threshold spin of $\chi_2 = 0.3$. Here, we assume a delay-time distribution with $n = 1$ and a minimal time delay of 10 Myr. The total merger rate in the local universe estimated by Abbott et al. (2016b) is shown as a square.

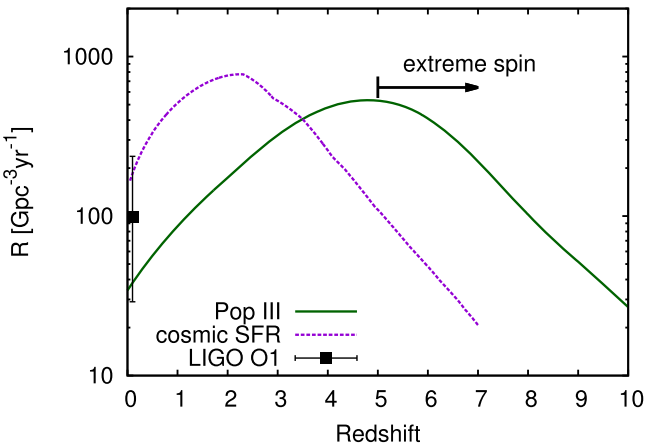

Figure 6. Same as Figure 5, but for the Pop III scenario. Also shown is the redshift evolution of the cosmic SFR scenario for a comparison. An arrow depicts the redshift where BBH mergers with extreme spins start to dominate the event rate.

Detmers et al. 2008). In this case, the synchronization time behaves as $\propto q^{-2}(a/R)^6$. This additional effect will speed up the synchronization. Note also that we have assumed circular orbits in this paper. One should use estimates of the synchronization time that include resonant excitations of g-modes, when considering elliptic orbits (Witte & Savonije 1999). However, these effects are beyond the scope of this paper. We will address this issue in a separate work.

The angular momentum loss due to winds is uncertain and it depends on the stellar metallicities. Although our results depend on the wind strength, the qualitative results in this paper are robust. Indeed, Zaldarriaga et al. (2017) show the robustness of this spin argument for WR progenitors for different wind parameters.

Mass loss and natal kick at the core collapse: We have assumed here that the mass of black holes is identical to that of the collapsing stars. This assumption is likely valid as long as the spin parameter of the progenitors does not exceed unity (O'Connor & Ott 2011; Sekiguchi & Shibata 2011). When the progenitor's spin exceeds unity, a fraction of the progenitor's mass is ejected, carrying the excess angular momentum, and hence the black hole has a mass smaller than the progenitor's (Barkov & Komissarov 2010). For WR stars, this effect is expected to be small because their maximal spin parameter does not significantly exceed unity.

One of the major concerns about the spin argument is that it is assumed that the direction of the spin angular momentum is parallel to the orbital angular momentum. This assumption is crucial because GW measurements are insensitive to spin parameters perpendicular to the orbital angular momentum. The tidal torque always works toward the orientation of the stellar spins that are parallel to the orbital angular momentum. Other effects of the binary interaction, e.g., mass transfer, also

change the spin components parallel to the orbital angular momentum. It has been suggested that the progenitor receives a natal kick during the core collapse (e.g., Janka 2013). This may cause a misalignment between the spin axes and the orbital axis. However, to significantly change the direction of the orbital angular momentum would require a kick $\gtrsim$500 km s^{-1}. Although such kicks have been observed at the high end of pulsar kicks, we do not expect such large natal kicks during black holes' formation. The fraction of the ejected mass to the remnant mass in this case is expected to be much smaller for black hole formation than the ratio in neutron star formation (see Janka 2013 and also Rodriguez et al. 2016b for a detailed study of the distributions $\chi_{\rm eff}$ including the natal kicks). Furthermore, observations of low-mass X-ray binaries show no evidence of strong natal kicks of black holes (see, e.g., Mandel 2016). These suggest typical values that are much smaller than the orbital velocities of the BBH progenitors. Therefore, we expect that BBH natal kicks may not affect significantly the spin components parallel to the orbital axis of the black holes, and hence the results of our analysis (see also discussions in Abbott et al. 2016a).

Mass transfer and common envelope phases: We considered two scenarios, (i) single synchronization and (ii) double synchronization. The spin of the black hole formed at the second core collapse of a binary is conserved as long as there is no significant mass accretion from the interstellar medium. Therefore, the spin parameters in the single synchronization case may be quite robust. On the other hand, the spin of the black hole formed at the first core collapse can change from the value at the birth of the black hole, due to mass accretion from the companion. Moreover, the semimajor axis may further change after the first core collapse, due to a common envelope phase. If this occurs, the spin parameter of this black hole has nothing to do with the initial semimajor axis of BBHs. Thus, the double synchronization case involves some uncertainties, or equivalently, the spin parameter of one of the black holes in BBH mergers is not well-constrained by the tidal synchronization argument.

Spin reduction due to the Blandford–Znajek process: One of the possible mechanisms powering GRB central engines is the Blanford–Znajek process, in which the rotational energy of a central black hole is removed through magnetic fields, and an ultra-relativistic jet is launched with this energy (Blandford & Znajek 1977). Although we still do not know whether or not this process works in collapsing massive stars, or what the effect of this process on the central black hole is, if this process removed a significant amount of the rotational energy, the spin of the black hole would be reduced.

9. Conclusions

The spins (projected on the orbital angular momentum axis) of the merging black holes observed by LIGO O1 run are rather small. We have examined the implications of these observations on the progenitor scenarios in which BBHs arise from isolated field binaries. Our analysis was done under the assumption that this projection indeed reflects the final spin of the progenitor star, just before it collapsed to a black hole. As the expected mass ejected during the formation of the black hole is rather small compared with the remnant black hole, we do not expect a strong natal kick, and hence a significant change in the black hole's spin or in the orbital angular momentum (see Rodriguez et al. 2016b for the effects of natal kicks on the effective spin parameters). With this assumption, we expect positive values of the aligned spin of BBH mergers in our scenario. Note that the dynamical capture scenario (Rodriguez et al. 2016b), the AGN scenario, and the cosmological scenario (Bird et al. 2016; Blinnikov et al. 2016) predict that half of BBH mergers have negative effective parameters (anti-aligned spin), so the detections of BBH mergers with negative spin parameters will support these scenarios.

We have studied the spin distribution and its redshift evolution based on the tidal synchronization argument (Kushnir et al. 2016). We find that for massive main-sequence progenitors, whose semimajor axes are small enough to merge within a Hubble time, the tidal synchronization occurs on timescales much shorter than their lifetime. As a result, the spin parameters of such main-sequence stars exceed unity. Given the fact that the aligned spin parameters of the three LIGO's O1 events measured via the GW signals are significantly less than unity, we can rule out the possibility that these BBHs are formed directly from the collapse of main-sequence stars. This also indicates that, if the BBHs formed via binary evolution beginning with two main-sequence stars, the progenitor binary systems must experience either a significant loss of their spin angular momentum (more than 95%) or a significant decrease in the semimajor axis during their evolution. This conclusion is consistent with current stellar and binary evolution studies (see, e.g., Belczynski et al. 2016).

Among known stellar objects, WR stars seem to be the only possible progenitors of the BBH mergers. We consider the spin distribution and redshift evolution of BBH mergers formed via WR progenitors, taking the synchronization, mass loss, and stellar lifetime into account. Here, we assume that the cosmic BBH formation history is proportional to either the cosmic SFR or to LGRB rate (LGRBs are also formed from WR stars) with two different delay-time distributions. We find that a steep delay-time distribution $\propto 1/t^2$ predicts too many BBH mergers with extreme spins $\chi \sim 1$. This is inconsistent with the LIGO's O1 events. On the contrary, for the delay-time distribution of $\propto 1/t$, the rate of BBH mergers with low spins ($\chi \lesssim 0.3$) dominates over the one with high spins ($\chi \gtrsim 0.3$) in the local universe. The ratio of high-spin mergers to the low-spin ones increases with the cosmological redshift and the high-spin population begins to dominate at a redshift of 0.5–1.5. This feature may be observable by GW detectors network in future.

The BBH merger rate density inferred from LIGO's O1 run is compatible with that of LGRBs. Motivated by this, we considered the possibility that BBH mergers and LGRBs share the same progenitors, i.e., that LGRBs are produced at the core collapse of stars in a close binary that eventually evolves to a BBH with a coalescence time of less than a Hubble time. We show that a stellar spin parameter of $\gtrsim$1.3, or equivalently, a coalescence time of $\lesssim$0.2 Gyr, is required for WR progenitors in order for a fraction of the stellar core to form an accretion disk around the central black hole. Assuming a delay-time distribution of $1/t$, with a minimal delay-time of 10 Myr, we expect that the LGRB rate is about one third of the BBH formation rate. Because BBHs with such extreme spins predominately merge at high redshifts, it is still possible that BBH mergers and LGRBs share the same progenitors, even though the aligned spin parameters of the LIGO's O1 events are significantly less than unity. We extrapolate the total BBH merger rate with low spins inferred from LIGO's O1 run to the

extreme spin population, based on the WR progenitor scenario, and show that the BBH merger rate with extreme spins is 20% of the total rate or less. This can be tested in the near future with further observations of BBH mergers.

We also considered the hypothetical Pop III BBH merger scenario. As these BBHs formed at high redshifts around $z \sim 10$, in the local universe, BBH mergers from Pop III stars always have a time delay of $\sim$10 Gyr. If they arise from synchronized stars, this corresponds to the BBH spin parameters of 0.2–0.6. However, it is not clear that these Pop III binaries are fully synchronized during their main-sequence phase, as the synchronization time is comparable to their lifetime. Furthermore, a fraction of the spin angular momentum may be removed during the stable mass transfer in the late phases, and this may reduce the spin parameters (see Inayoshi et al. 2017). Therefore, we conclude that the Pop III star scenario could be consistent with the low aligned spins of the three LIGO's O1 events. In this scenario, the BBH merger rate increases with the redshift up to $z \sim 5$, and we expect BBH merges with extreme spins beyond a redshift of 4. These are unique observable features of this scenario.

To summarize, we have shown that the low aligned spins of the BBH mergers observed in LIGO's O1 run are consistent with WR progenitors. Those are also progenitors of LGRBs; given the comparable observed rate, it might be that LGRBs arise when the WR progenitors collapse to form the observed BBHs. Although the observed spins are slightly lower than expected, Pop III stars cannot be ruled out either. Both scenarios predict that some high-aligned-spin BBHs should be discovered as well. If these are not discovered within LIGO's coming runs, then the observations will imply that it is unlikely that LIGO's BBHs have been formed via regular binary stellar evolution channels, and thus, the capture in dense environments (clusters or galactic cores) of primordial origin will be preferred.

We thank Maxim Barkov, Matteo Cantiello, Sivan Ginzburg, James Guillochon, Kohei Inayoshi, Tomoya Kinugawa, Itai Linial, Masaru Shibata, Maurice van Putten, and Roni Waldman for useful discussions and comments. K.H. is supported by the Flatiron Fellowship at the Simons Foundation. This research was supported by an advanced ERC grant TReX and by the ISF-CHE I-Core center of excellence for research in Astrophysics.

References

Abbott, B. P., Abbott, R., Abbott, T. D., et al. 2016a, ApJL, 818, L22
Abbott, B. P., Abbott, R., Abbott, T. D., et al. 2016b, PhRvX, 6, 041015
Abbott, B. P., Abbott, R., Abbott, T. D., et al. 2016c, PhRvL, 116, 061102
Antonini, F., & Rasio, F. A. 2016, ApJ, 831, 187
Barkov, M. V., & Komissarov, S. S. 2010, MNRAS, 401, 1644
Bartos, I., Kocsis, B., Haiman, Z., & Márka, S. 2017, ApJ, 835, 165
Belczynski, K., Holz, D. E., Bulik, T., & O'Shaughnessy, R. 2016, Natur, 534, 512
Bird, S., Cholis, I., Muñoz, J. B., et al. 2016, PhRvL, 116, 201301
Blandford, R. D., & Znajek, R. L. 1977, MNRAS, 179, 433
Blinnikov, S., Dolgov, A., Porayko, N. K., & Postnov, K. 2016, JCAP, 11, 036
Bromberg, O., Nakar, E., Piran, T., & Sari, R. 2011, ApJ, 740, 100
Bromberg, O., Nakar, E., Piran, T., & Sari, R. 2012, ApJ, 749, 110
Bulik, T., Belczynski, K., & Prestwich, A. 2011, ApJ, 730, 140
Carpano, S., Pollock, A. M. T., Prestwich, A., et al. 2007, A&A, 466, L17
Crowther, P. A., Barnard, R., Carpano, S., et al. 2010, MNRAS, 403, L41
de Souza, R. S., Yoshida, N., & Ioka, K. 2011, A&A, 533, A32
Detmers, R. G., Langer, N., Podsiadlowski, P., & Izzard, R. G. 2008, A&A, 484, 831
Eggleton, P. P. 1983, ApJ, 268, 368
Esposito, P., Israel, G. L., Milisavljevic, D., et al. 2015, MNRAS, 452, 1112
Farr, W. M., Sravan, N., Cantrell, A., et al. 2011, ApJ, 741, 103
Ghirlanda, G., Salafia, O. S., Pescalli, A., et al. 2016, A&A, 594, A84
Goldreich, P., & Nicholson, P. D. 1989, ApJ, 342, 1079
Hirano, S., Hosokawa, T., Yoshida, N., et al. 2014, ApJ, 781, 60
Hirschi, R., Meynet, G., & Maeder, A. 2004, A&A, 425, 649
Hosokawa, T., Omukai, K., Yoshida, N., & Yorke, H. W. 2011, Sci, 334, 1250
Hurley, J. R., Pols, O. R., & Tout, C. A. 2000, MNRAS, 315, 543
Inayoshi, K., Hirai, R., Kinugawa, T., & Hotokezaka, K. 2017, arXiv:1701.04823
Ioka, K., Chiba, T., Tanaka, T., & Nakamura, T. 1998, PhRvD, 58, 063003
Ivanova, N., Justham, S., Chen, X., et al. 2013, A&ARv, 21, 59
Janka, H.-T. 2013, MNRAS, 434, 1355
Kashlinsky, A. 2016, ApJL, 823, L25
Kinugawa, T., Inayoshi, K., Hotokezaka, K., Nakauchi, D., & Nakamura, T. 2014, MNRAS, 442, 2963
Kruckow, M. U., Tauris, T. M., Langer, N., et al. 2016, A&A, 596, A58
Kushnir, D., Zaldarriaga, M., Kollmeier, J. A., & Waldman, R. 2016, MNRAS, 462, 844
Kushnir, D., Zaldarriaga, M., Kollmeier, J. A., & Waldman, R. 2017, MNRAS, 467, 2146
Langer, N., Hamann, W.-R., Lennon, M., et al. 1994, A&A, 290, 819
Liu, J.-F., Bregman, J. N., Bai, Y., Justham, S., & Crowther, P. 2013, Natur, 503, 500
MacFadyen, A. I., & Woosley, S. E. 1999, ApJ, 524, 262
Madau, P., & Dickinson, M. 2014, ARA&A, 52, 415
Mandel, I. 2016, MNRAS, 456, 578
Mandel, I., & de Mink, S. E. 2016, MNRAS, 458, 2634
Maoz, D., Mannucci, F., & Nelemans, G. 2014, ARA&A, 52, 107
Marchant, P., Langer, N., Podsiadlowski, P., Tauris, T. M., & Moriya, T. J. 2016, A&A, 588, A50
Marigo, P., Girardi, L., Chiosi, C., & Wood, P. R. 2001, A&A, 371, 152
Meynet, G., Georgy, C., Hirschi, R., et al. 2011, BSRSL, 80, 266
Meynet, G., & Maeder, A. 2003, A&A, 404, 975
Meynet, G., & Maeder, A. 2005, A&A, 429, 581
Meynet, G., & Maeder, A. 2007, A&A, 464, L11
Nakamura, T., Ando, M., Kinugawa, T., et al. 2016, PTEP, 2016, 093E01
O'Connor, E., & Ott, C. D. 2011, ApJ, 730, 70
O'Leary, R. M., Meiron, Y., & Kocsis, B. 2016, ApJL, 824, L12
Omukai, K., & Palla, F. 2003, ApJ, 589, 677
Özel, F., Psaltis, D., Narayan, R., & McClintock, J. E. 2010, ApJ, 725, 1918
Peters, P. C. 1964, PhRv, 136, 1224
Podsiadlowski, P., Mazzali, P. A., Nomoto, K., Lazzati, D., & Cappellaro, E. 2004, ApJL, 607, L17
Prestwich, A. H., Kilgard, R., Crowther, P. A., et al. 2007, ApJL, 669, L21
Ramírez-Agudelo, O. H., Sana, H., de Mink, S. E., et al. 2015, A&A, 580, A92
Rodriguez, C. L., Haster, C.-J., Chatterjee, S., Kalogera, V., & Rasio, F. A. 2016a, ApJL, 824, L8
Rodriguez, C. L., Zevin, M., Pankow, C., Kalogera, V., & Rasio, F. A. 2016b, ApJL, 832, L2
Sasaki, M., Suyama, T., Tanaka, T., & Yokoyama, S. 2016, PhRvL, 117, 061101
Sekiguchi, Y., & Shibata, M. 2011, ApJ, 737, 6
Silverman, J. M., & Filippenko, A. V. 2008, ApJL, 678, L17
Stone, N. C., Metzger, B. D., & Haiman, Z. 2017, MNRAS, 464, 946
Toledano, O., Moreno, E., Koenigsberger, G., Detmers, R., & Langer, N. 2007, A&A, 461, 1057
Tout, C. A., Pols, O. R., Eggleton, P. P., & Han, Z. 1996, MNRAS, 281, 257
Ud-Doula, A., Owocki, S. P., & Townsend, R. H. D. 2009, MNRAS, 392, 1022
van den Heuvel, E. P. J., Portegies Zwart, S. F., & de Mink, S. E. 2017, arXiv:1701.02355
Visbal, E., Haiman, Z., & Bryan, G. L. 2015, MNRAS, 453, 4456
Wanderman, D., & Piran, T. 2010, MNRAS, 406, 1944
Witte, M. G., & Savonije, G. J. 1999, A&A, 350, 129
Woosley, S. E. 1993, ApJ, 405, 273
Woosley, S. E., & Heger, A. 2012, ApJ, 752, 32
Zahn, J.-P. 1975, A&A, 41, 329
Zahn, J.-P. 1977, A&A, 57, 383
Zaldarriaga, M., Kushnir, D., & Kollmeier, J. A. 2017, arXiv:1702.00885